This article has been accepted for publication in IEEE Transactions on Green Communications and Networking. This is the author's version which has not been fully edited and content may change prior to final publication. Citation information: DOI 10.1109/TGCN.2023.3238176

Reconfigurable Adaptive Channel Sensing

Manuj Mukherjee† Aslan Tchamkerten* Chadi Jabbour*

***Abstract*—This paper proposes an energy-efficient detection scheme, referred to as AdaSense, that is particularly suitable in the sparse regime when events to be detected happen rarely. To minimize energy consumption, AdaSense exploits the dependency between the receiver noise figure (*i.e.*, the receiver added noise) and the receiver power consumption; less noisy channel observations typically imply higher power consumption.**

AdaSense is duty-cycled and begins each cycle with a few channel observations in a low-power-low-reliability mode. Based on these observations, it makes a first tentative decision on whether or not a message is present. If no message is declared, AdaSense waits till the beginning of the next cycle and starts afresh. If a message is tentatively declared, AdaSense enters a confirmation second phase, takes more samples, but now in a high-power-high-reliability mode. If these observations confirm the tentative decision, AdaSense stops, else AdaSense waits till the beginning of the next cycle and starts afresh in the low-power-low-reliability mode.

Compared to prominent detection schemes such as the clear channel assessment algorithm of the Berkeley Media Access Control (BMAC) protocol, AdaSense provides relative energy gains that grow unbounded in the small probability of false-alarm regime, as communication gets sparser. In the non-asymptotic regime, energy gains are 30% to 75% for communication scenarios typically found in the context of wake-up receivers.

***Index Terms*—Channel sensing, detection, adaptive sampling, low-energy communication, wake-up receiver**

I. Introduction

Event-triggered communication scenarios, such as alarms and monitoring systems [1]–[3], or distributed detection in wireless sensor networks [4]–[6], often arise in the context of device-to-device communication. Predominantly, these devices possess limited battery [7]. Consequently, keeping these devices constantly switched-on is infeasible, especially if the event triggering the communication is low-probability, such as fire alarms [8].

To minimize energy consumption modern receivers are typically *duty cycled* [9]–[17], *i.e.*, they listen only at predetermined time periods, and sleep otherwise. To alert the receiver of an incoming message, the transmitter sends a preamble either at the beginning of a listening period (*e.g.*, [9], [17]–[19]), or immediately in which case the preamble is long enough to cover at least one listening period (*e.g.*, [12], [15]). In both cases (as seen in [9], [12], [15], [17]–[19]) the receiver performs a binary hypothesis test, referred to as *channel sensing*, during the listening periods, to decide whether or not a preamble is present.

* A. Tchamkerten and C. Jabbour are with Telecom Paris, Institut Polytechnique de Paris, France. Email: {aslan.tchamkerten, chadi.jabbour}@telecom-paris.fr.

† M. Mukherjee is with the Indraprastha Institute of Information Technology Delhi, India. Email: manuj@iiitd.ac.in

How to minimize the energy consumption of a channel sensing scheme given a desired reliability specified in terms of the probabilities of false-alarm and miss-detection? In this paper we address this question through a simple scheme referred to as AdaSense (for adaptive sensing). In a nutshell, AdaSense reconfigures its noise level in an adaptive manner in order to strike a balance between reliability and energy consumption. In more detail, the significant contributor to the noise in a machine-to-machine communication channel is the receiver noise, which is typically a non-increasing function of the power consumption at the receiver (see, *e.g.*, [20, Chapter 12]); therefore, higher reliability requires greater power consumption. AdaSense exploits this dependency to adaptively choose the noise level of the observed samples in order to minimize the overall energy consumed in channel sensing.

AdaSense has two phases. In the first phase, AdaSense observes a small batch of samples at low power and makes a tentative decision on whether or not a preamble is present. If no preamble is detected, AdaSense stops, declares that there is no preamble, and moves to the next listening phase. If a preamble is detected, AdaSense enters a second confirmation phase and observes a fresh batch of samples at a higher power. At the end of this second phase, AdaSense decides whether or not the preamble is present. An overview of AdaSense's operation is available in Figure 1.

We compared AdaSense against two well-known schemes, the "single-phase" scheme and the *clear channel assessment algorithm* of the *Berkeley Media Access Control* (BMAC) protocol [12], henceforth referred to as the BMAC scheme. The single-phase scheme refers to the standard binary hypothesis test based on the observations at constant power of a fixed number of n samples, where n denotes the length of the preamble. Upon observation, either a preamble is declared, or otherwise the receiver stops and waits for the next listening period. The BMAC scheme instead is sequential. The receiver observes samples at a constant power and declares that the preamble is present only if all n sample values exceed a given threshold. As soon as one sample value is below the threshold, it stops, declares that no preamble is present, and waits for the next listening period.

We show that the relative energy gain of AdaSense, compared to the BMAC and the single-phase schemes, grow unbounded in the small probability of false alarm regime. In the non-asymptotic setting, our comparisons demonstrate that AdaSense achieves the targeted sensing performance with a reduced detection time, while consuming 30%-75% less energy than the single-phase and the BMAC schemes, across communication scenarios typically encountered in the context of event-triggered communication.

This article has been accepted for publication in IEEE Transactions on Green Communications and Networking. This is the author's version which has not been fully edited and content may change prior to final publication. Citation information: DOI 10.1109/TGCN.2023.3238176

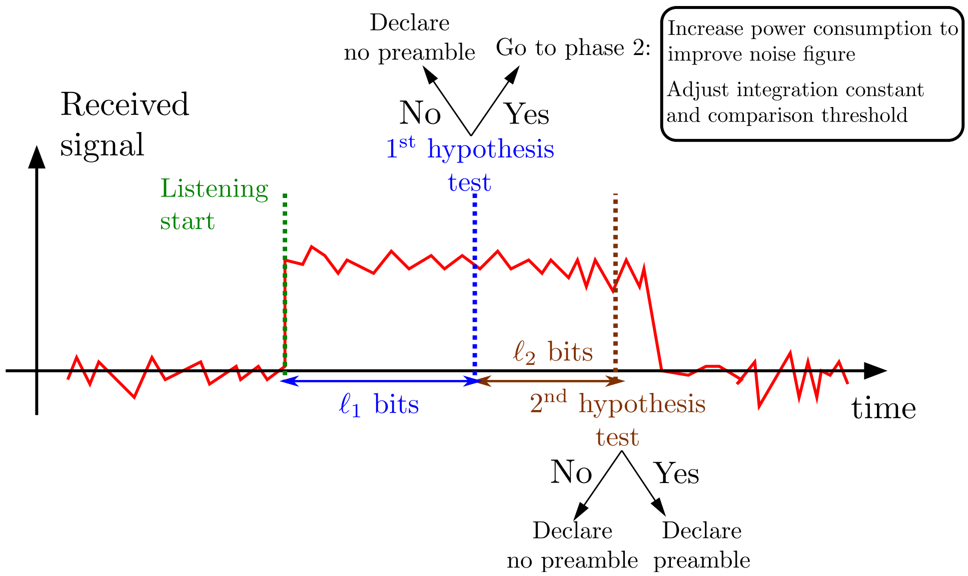

Fig. 1: An overview of AdaSense

A. Related works

AdaSense is inspired by the adaptive detection schemes proposed in [21]–[24] which aim at minimizing the number of samples needed to efficiently detect a message. While the number of samples can be taken as a proxy for energy consumption, the present paper goes further by considering the actual energy spent in the observation of a sample through its dependency with the receiver noise figure. In particular, leveraging upon this dependency AdaSense adaptively varies the power consumption, in addition to the number of samples.

Two-stage detection schemes have also been proposed in the context of cognitive radios, where a binary hypothesis test is performed to determine whether a channel is busy or free [25]–[27].[1] These schemes however are weaker than AdaSense, since they only vary detection thresholds across the two phases, while keeping the power consumption constant. Moreover, the number of samples observed in the different phases are fixed beforehand, irrespective of the targeted levels of reliability. In contrast, AdaSense saves energy by choosing a different power consumption and a different number of samples for the two phases according to the desired reliability level.

B. Organization

The rest of the paper is organized as follows. In Section II, we give a precise description of the channel sensing problem. In Section III, we describe AdaSense and compare it with the single-phase scheme and the BMAC scheme. We first make analytical comparisons in the small probability of false-alarm regime as communication gets sparser, then make comparisons in non-asymptotic regimes through numerical performance evaluations. In Section IV, we discuss a possible practical implementation of AdaSense. Finally, in Section V, we draw a few concluding remarks.

[1] One should note that these schemes use a *non-coherent receiver*, and hence the observed statistic on which they perform the hypothesis test is the signal energy. This is in contrast to our setting which involve coherent receivers (see Section II), and hence we observe the signal directly. However, adapting the detection schemes of [25]–[27] to our setting is straightforward.

II. Channel Sensing: Reliability and Energy Consumption

Channel sensing at the physical layer amounts to a binary hypothesis test. Let $Y_1, Y_2, \ldots, Y_N$ denote the outputs of a coherent receiver that observes a modulated binary message $M \in \{0,1\}$, repeated N times, and corrupted by additive noise, that is

$$Y_i = M \cdot \sqrt{P} + Z_i, \;\; 1 \le i \le N, \tag{1}$$

where $Z_i \sim \mathcal{N}(0, \sigma_i^2)$ denotes the noise of the i-th sample, and where P denotes the received power.[2]

The two possible values of M are interpreted as the hypothesis $H_0 = \{M = 0\}$, corresponding to no preamble, and $H_1 = \{M = 1\}$, corresponding to a preamble being present. These hypothesis are supposed to have a known prior which reflects the level of communication sparsity

$$p_1 = \Pr(H_1) = 1 - \Pr(H_0).$$

Based on $Y_1, Y_2, \ldots, Y_N$ the receiver provides a message estimate $\widehat{M} \in \{0,1\}$. The reliability of the estimator is quantified in terms of the probabilities of false-alarm and miss-detection

$$\begin{aligned} P_{\text{FA}} &= \Pr(\widehat{M} = 1 | H_0) \\ P_{\text{Miss}} &= \Pr(\widehat{M} = 0 | H_1). \end{aligned} \tag{2}$$

In addition to reliability, we are interested in the average energy E spent by the receiver in observing $Y_1, \ldots, Y_N$. To

[2] $\mathcal{N}(\mu, \sigma^2)$ refers to the Gaussian distribution with mean μ and variance σ^2.

quantify this energy, observe that the noise variance σ_i^2 may be decomposed as

$$\sigma_i^2 = \sigma_t^2 + \sigma_{r,i}^2,$$

where σ_t^2 denotes the contribution due to thermal noise, and where $\sigma_{r,i}^2$ denotes the contribution of the receiver. In many practical setups (see Section III-C), the thermal noise σ_t^2 is negligible with respect to the receiver noise and is thus ignored. Therefore, we assume that

$$\sigma_i^2 = \sigma_{r,i}^2.$$

Our results (next section) immediately extend to the case where σ_t^2 is no longer negligible, but yield slightly more cumbersome analytical results—this is briefly alluded to in Section V.

The receiver noise variance $\sigma_{r,i}^2$ is typically a function of the receiver power consumption $P_{r,i}$; the lower $\sigma_{r,i}^2$ the larger $P_{r,i}$. This function depends on the receiver circuit itself, and particularly on the low noise amplifier used in the receiver circuit (see, *e.g.*, [20, Chapter 12]). We model this dependency by letting

$$\sigma_{r,i}^2 = f(P_{r,i})$$

where $f(\cdot)$ denotes a non-negative and non-increasing function, which we shall refer to as the *noise profile* of the receiver—in practice this function can be determined by means of electrical simulations on the low noise amplifier.[3] Based on [28], throughout the paper we assume that the noise profile is given by

$$\sigma_{r,i}^2 = kP_{r,i}^{-\gamma}$$

for some known $k > 0$ and $\gamma \geq 1$—the case $\gamma < 1$ is arguably less natural and shall be omitted.

Without loss of generality, we assume that the number of observed samples, N, is no larger than the length n of the preamble. Moreover, both the number of observed samples and the power at which the samples are observed can be chosen adaptively. In more detail, the decision to stop at the i-th observation may depend on $Y_1, \ldots, Y_i$. Similarly, the power $P_{r,i}$ at which symbol Y_i is observed may depend on past observed samples $Y_1, Y_2, \ldots, Y_{i-1}$. In probability language, N is a stopping time [29, Chapter 9] defined on the natural filtration induced by the process $Y_1, Y_2, \ldots$, and the process $P_{r,1}, P_{r,2}, \ldots$ is predictable with respect to this filtration.

The average energy consumption till a decision is made is then given by

$$E = \mathbb{E}\left(\sum_{i=1}^{N} P_{r,i}\right) \tag{3}$$

where $\mathbb{E}$ denotes expectation over the channel noise and over the two hypothesis H_1 and H_0, assumed to have prior p_1 and $1 - p_1$, respectively. Here, we assume that each symbol has unit duration, without loss of generality.[4]

[3]We emphasize the distinction between P, the power of the received signal, and P_r the power consumed by the receiver to observe the signal.

[4]For an arbitrary symbol duration T_s, just multiply E by T_s in equation (3).

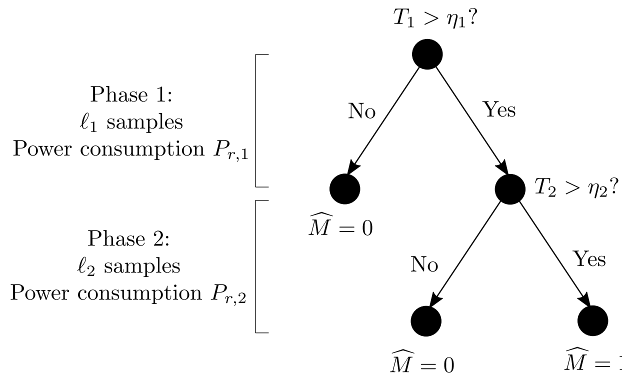

Fig. 2: Two-stage decision procedure of AdaSense.

III. Results

We first describe *AdaSense* in Section III-A, a scheme which aims at minimizing E for fixed P_{FA} and P_{Miss}. We then compare AdaSense against two well-known detection schemes, namely the single-phase scheme and the BMAC scheme. In Section III-B, we provide analytical comparisons in the regime of small probability of false-alarm and sparse communication, which is relevant for IoT type of applications. In Section III-C, we numerically compare these schemes for a variety of relevant non-asymptotic parameters.

A. AdaSense

AdaSense is a two-phase scheme as illustrated in Fig. 2. It starts by observing a first batch of samples and makes a tentative decision. If H_0 is declared AdaSense stops, and if H_1 is declared AdaSense performs a second "highly reliable" confirmation test based on a second batch of samples. If hypothesis H_1 is confirmed, AdaSense outputs H_1, else it outputs H_0.

In more detail, let ℓ_1 and ℓ_2 be two nonnegative integers such that $\ell_1 + \ell_2 \leq n$, and let $P_{r,1}, P_{r,2}$ be the receiver power consumptions for the two phases. The receiver starts by observing ℓ_1 samples $Y_1, Y_2, \cdots, Y_{\ell_1}$ at a constant power $P_{r,1}$ per sample . It then performs a standard log-likelihood ratio (LLR) test to discriminate between the hypothesis H_0 and H_1 (see Case III.B.2 of [30]), *i.e.*, the receiver checks whether

$$T_1 \triangleq \frac{\sqrt{P}}{\sigma_{r,1}^2}\sum_{i=1}^{\ell_1} Y_i - \frac{\ell_1 P}{2\sigma_{r,1}^2} \leq \eta_1, \tag{4}$$

for some given threshold η_1, and where $\sigma_{r,1}^2 = f(P_{r,1})$. If this inequality is satisfied, the receiver stops and declares $\widehat{M} = 0$. Otherwise, it enters a second confirmation phase, observes the next ℓ_2 samples $Y_{\ell_1+1}, \ldots, Y_{\ell_1+\ell_2}$ at a constant power $P_{r,2}$ per sample, typically greater than $P_{r,1}$, and performs a second LLR test on this second batch of samples, *i.e.*, it checks whether

$$T_2 \triangleq \frac{\sqrt{P}}{\sigma_{r,2}^2}\sum_{i=\ell_1+1}^{\ell_1+\ell_2} Y_i - \frac{\ell_2 P}{2\sigma_{r,2}^2} > \eta_2 \tag{5}$$

for some given threshold η_2, and where $\sigma_{r,2}^2 = f(P_{r,2})$. If this second inequality is satisfied, the receiver declares $\widehat{M} = 1$, and otherwise $\widehat{M} = 0$.

For this scheme, P_{FA}, P_{Miss} and E are explicitly given by (see Appendix A)[5]

$$P_{\text{FA}} = Q\left(\frac{\sigma_{r,1}\eta_1}{\sqrt{\ell_1 P}} + \frac{1}{2}\sqrt{\frac{\ell_1 P}{\sigma_{r,1}^2}}\right) Q\left(\frac{\sigma_{r,2}\eta_2}{\sqrt{\ell_2 P}} + \frac{1}{2}\sqrt{\frac{\ell_2 P}{\sigma_{r,2}^2}}\right), \quad (6)$$

$$\begin{aligned} P_{\text{Miss}} = Q&\left(-\frac{\sigma_{r,1}\eta_1}{\sqrt{\ell_1 P}} + \frac{1}{2}\sqrt{\frac{\ell_1 P}{\sigma_{r,1}^2}}\right) \\ &+ \left(1 - Q\left(-\frac{\sigma_{r,1}\eta_1}{\sqrt{\ell_1 P}} + \frac{1}{2}\sqrt{\frac{\ell_1 P}{\sigma_{r,1}^2}}\right)\right) \\ &\quad \times Q\left(-\frac{\sigma_{r,2}\eta_2}{\sqrt{\ell_2 P}} + \frac{1}{2}\sqrt{\frac{\ell_2 P}{\sigma_{r,2}^2}}\right), \end{aligned} \quad (7)$$

and

$$E = \ell_1 P_{r,1} + p_c \ell_2 P_{r,2}, \quad (8)$$

where p_c denotes the probability of having a second phase and is given by

$$\begin{aligned} p_c \triangleq (1-p_1) Q&\left(\frac{\sigma_{r,1}\eta_1}{\sqrt{\ell_1 P}} + \frac{1}{2}\sqrt{\frac{\ell_1 P}{\sigma_{r,1}^2}}\right) \\ &+ p_1\left(1 - Q\left(-\frac{\sigma_{r,1}\eta_1}{\sqrt{\ell_1 P}} + \frac{1}{2}\sqrt{\frac{\ell_1 P}{\sigma_{r,1}^2}}\right)\right). \end{aligned}$$

Given the received power P, the preamble length n, the sparsity level p_1, and the reliability targets $P_{\text{FA}} \leq \alpha$, $P_{\text{Miss}} \leq \beta$, the set of parameters $\{\ell_1, P_{r,1}, \eta_1, \ell_2, P_{r,2}, \eta_2\}$ are chosen so that to minimize the average energy:

$$\{\ell_1^*, P_{r,1}^*, \eta_1^*, \ell_2^*, P_{r,2}^*, \eta_2^*\} = \underset{\substack{\{\ell_1, P_{r,1}, \eta_1, \ell_2, P_{r,2}, \eta_2\}: \\ \ell_1+\ell_2 \leq n \\ P_{\text{FA}} \leq \alpha \\ P_{\text{Miss}} \leq \beta}}{\arg\min} E. \quad (9)$$

Note that N takes value ℓ_1 or $\ell_1 + \ell_2$ and that the constraint $\ell_1 + \ell_2 \leq n$ refers to the constraint $N \leq n$—see Section II.

The optimization problem in (9) is non-convex. A quick way to see this is as follows. Consider the constraint $P_{\text{Miss}} \leq \beta$. Note that the expression for P_{Miss} given in (7) involves Q-functions which are non-convex. Furthermore, observe that the variable ℓ_1 appears within the argument to Q-functions present in the constraint in the following way, $Q(\frac{a}{\sqrt{\ell_1}} + b\sqrt{\ell_1})$. Again, it is not difficult to see that functions of the form $f(x) = \frac{a}{\sqrt{x}} + b\sqrt{x}$ are not convex in general. As a result the constraint $P_{\text{Miss}} \leq \beta$ is clearly a non-convex constraint. One can similarly argue using (6) and (8) respectively that the constraint $P_{\text{FA}} \leq \alpha$ and the objective function E (due to the presence of the quantity p_c) are non-convex.

It is well-known that non-convex optimization admits no analytical solution in general (see for example Section 1.4 of [31]). Fortunately, for our purpose, the optimization problem (9) can easily be numerically evaluated as described in Section III-C. It should also be noted that this optimization needs to be carried only once per target values α, β, n, p_1 and P. Depending on (n, α, β) there might be no solution[6] in which case we set $E = \infty$. However, if only (α, β) are fixed and n can be optimized over then the above optimization problem always admits a feasible solution (see, *e.g.*, [30, Example II.D.1]).

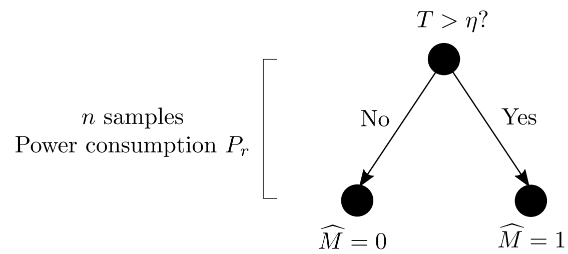

Fig. 3: Single-phase scheme

B. Performance: Small probability of False-Alarm and Sparse Communication regime

The next result explicits a tradeoff between E and P_{FA} at fixed P_{Miss} for AdaSense, when P_{FA} tends to zero (the proof is deferred to Appendix C):[7]

Theorem 1 (AdaSense, asymptotics)**.** *Suppose $f(P_r) = kP_r^{-\gamma}$ for some fixed $\gamma \geq 1$ and $k > 0$. For any fixed $p_1, P > 0$, $0 < \beta \leq 1$ and $0 < \varepsilon < 1$ AdaSense achieves $P_{\textit{Miss}} \leq \beta$ and*

$$E \leq \frac{2kp_1}{P(1-\varepsilon - o(1))} \ln\left(\frac{1}{P_{\textit{FA}}}\right) \quad (10)$$

where $o(1) \to 0$ as $P_{\textit{FA}} \to 0$. Moreover, this tradeoff between $P_{\textit{Miss}}$, $P_{\textit{FA}}$, and E is achievable with $n = O(\ln(1/P_{\textit{FA}}))$.

The important thing to notice here is that the sparser the communication, that is the smaller p_1, the lower E. To put this result into perspective we now consider two other widely known detection schemes, namely the basic "single-phase" scheme and the BMAC scheme.

The single-phase scheme is described in Fig. 3. The receiver performs an (optimal) LLR test on a fixed number of n samples $Y_1, \ldots, Y_n$, each observed at a constant receiver power P_r. The test consists in declaring $\widehat{M} = 1$ whenever $T \triangleq \frac{\sqrt{P}}{\sigma_r^2} \sum_{i=1}^n Y_i - \frac{nP}{2\sigma_r^2}$ is above a given threshold η that depends on the probability of false-alarm, and $\widehat{M} = 0$ otherwise. The following theorem, which is essentially a direct consequence of Stein's Lemma [32, Theorem 11.8.3] (see Appendix C for the proof), states the performance of the single-phase scheme in the small probability of false-alarm regime:

Theorem 2 (Single-phase, asymptotics)**.** *Suppose $\sigma_r^2 = f(P_r) = kP_r^{-\gamma}$ for some fixed $\gamma \geq 1$ and $k > 0$. For*

[5] Q refers to the standard Q-function defined as $Q(x) = \frac{1}{\sqrt{2\pi}} \int_x^\infty e^{-\frac{u^2}{2}} du$.

[6] That is no $\{\ell_1, P_{r,1}, \eta_1, \ell_2, P_{r,2}, \eta_2\}$ such that $\ell_1 + \ell_2 \leq n$, $P_{\text{FA}} \leq \alpha$, and $P_{\text{Miss}} \leq \beta$

[7] We make use of the Big O notation for limiting function behavior.

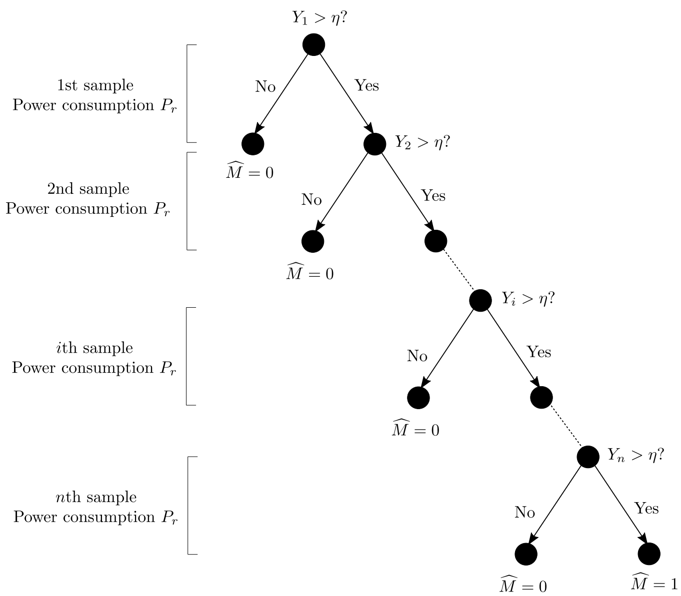

Fig. 4: BMAC scheme

fixed $p_1, P, P_r > 0$ *and* $0 < \beta \leq 1$ *the single-phase scheme achieves* $P_{Miss} \leq \beta$ *and*

$$E = \frac{2k}{P P_r^{\gamma-1}(1 \pm o(1))} \ln\left(\frac{1}{P_{FA}}\right)$$

with a preamble length $n = O(\ln(1/P_{FA}))$, *and where* $o(1)$ *vanishes as* $P_{FA} \to 0$.

By contrast with AdaSense, here E does not decrease as communication gets sparser (*i.e.*, as p_1 decreases).

An alternative scheme is the well-known BMAC scheme of [12] and described in Fig. 4. Similarly to the single-phase scheme, the receiver operates at a constant power. But instead of performing a hypothesis test based on all samples $Y_1, \ldots, Y_n$, the receiver performs a binary hypothesis test sequentially and independently on the Y_i's and declares $\widehat{M} = 0$ as soon as it finds a sample $Y_i \leq \eta$, where η depends on the probability of false-alarm. If all n samples exceed η, the receiver declares $\widehat{M} = 1$.

The following theorem characterizes the performance of the BMAC scheme in the low probability of false-alarm regime (the proof is deferred to Appendix C):

Theorem 3 (BMAC, asymptotics)**.** *Suppose* $\sigma_r^2 = f(P_r) = kP_r^{-\gamma}$ *for some fixed* $\gamma \geq 1$ *and* $k > 0$. *For any fixed* $p_1, P > 0$, $n \geq 1$ *and* $0 < \beta \leq 1$ *the BMAC scheme achieves* $P_{Miss} \leq \beta$ *and*

$$E \geq (1 - p_1)\left(\frac{2k}{nP} \ln\left(\frac{1}{P_{FA}}\right)\right)^{1/\gamma}(1 - o(1))$$

where $o(1) \to 0$ *as* $P_{FA} \to 0$.

Similarly to the single-phase scheme, the energy spent by the BMAC scheme does not decrease as communication gets sparser. But note that the above lower bound has the preamble length n in the denominator. It turns out that this is inherent to the BMAC scheme and is not due to a loose lower bound—see proof of Theorem 3. A larger value of n allows to lower the receiver power for a given level of false-alarm. However, if we impose BMAC to operate with the same preamble length as for AdaSense, and require $n = O(\ln(1/P_{\text{FA}}))$, AdaSense remains the most energy efficient in the sparse regime $p_1 \to 0$, at a fixed but small probability of false-alarm. In the next section, we will also see that for a wide range of parameter values AdaSense performs the best in terms of energy consumption.

C. Performance: Nonasymptotic Parameters regime

In this section we compare the performances of AdaSense, BMAC, and the single-phase scheme with parameters found in the context of wake-up receivers. Regarding preamble length we consider $n \in \{20, 30, 40, 50\}$ which are consistent with the value in [14]. We fix the range of target P_{FA} and P_{Miss} to be respectively $[10^{-6}, 10^{-3}]$ and $[10^{-10}, 10^{-3}]$, as in [14], [33].

The probability p_1 varies with applications. For example, temperature sensors deployed in some cities are monitored every few minutes [34], which, considering a standard bit rate of 100 kbps and $n = 50$, corresponds to $p_1 = 10^{-6}$. For other applications, for example fire alarms, p_1 can be much lower (see *e.g.*, [8]).

A survey published in 2017 [28] recommends a worst-case received power of -83 dBm, which corresponds to a line-of-sight communication over 1200 m using an antenna transmitting at 10 mW. Accordingly, we carry out the comparisons for values of received power in the range $P \in [-60$ dBm, -80 dBm$]$.

The noise profile, *i.e.*, the function that relates the power consumption to the receiver noise variance, is unique to each receiver, and is determined by electrical simulations performed on the low noise amplifier to be used at the input stage of the receiver. For demonstration purposes, we use the noise profile determined in [28, Section V.B] by stating the tradeoff between *sensitivity* and power consumption. Sensitivity is the defined as the received power needed to detect a single bit with a bit error rate of 10^{-3} [35]. It is a textbook result that an SNR of 15 dB is needed to detect a single bit with a bit error rate of 10^{-3} (see [30, Example II.B.2]), and hence, receiver noise power is simply sensitivity lowered by 15 dB. The sensitivity versus power consumption tradeoff mentioned in the survey can then be rephrased as follows: 1 μW of power consumption leads to a receiver noise of -55 dBm, and the noise power is decreased by 20 dB by increasing the power consumption ten times. This tradeoff corresponds to the noise profile $f(\cdot)$ given by

$$\sigma_r^2 = f(P_r) = \frac{10^{-20.5}}{P_r^2},$$

where P_r is in Watts. The contribution of the thermal noise to the overall noise power is negligible, since the least value of σ_r^2 used in our comparisons is -92.15 dBm, whereas standard values of thermal noise power lie below -113.83 dBm.[8]

[8]The thermal noise power is calculated using the formula $\sigma_t^2 = k_b T B$ in Watts [20, Chapter 11], where k_b is the Boltzman constant, T is the temperature, and B is the bandwidth. We have used $T = 300$K (see for example [35]) and $B = 1$MHz, which is the maximum bandwidth allocated to low power devices in the IEEE 802.15.4 standard for low-rate communication [36].

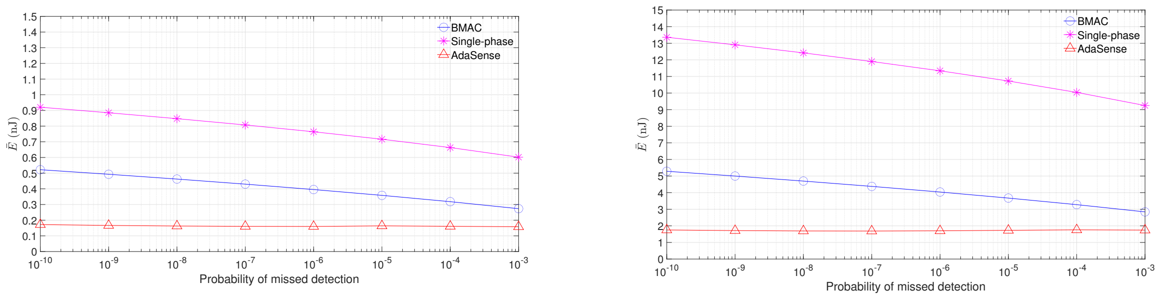

(a) $n = 30$, $P = -60$ dBm, $P_{\text{FA}} = 10^{-3}$. Energy savings 43%-67%.

(b) $n = 50$, $P = -80$ dBm, $P_{\text{FA}} = 10^{-5}$. Energy savings 39%-67%.

Fig. 5: E versus P_{Miss} for the three different schemes with $p_1 = 10^{-10}$ and under two different regimes of P, n, and P_{FA}.

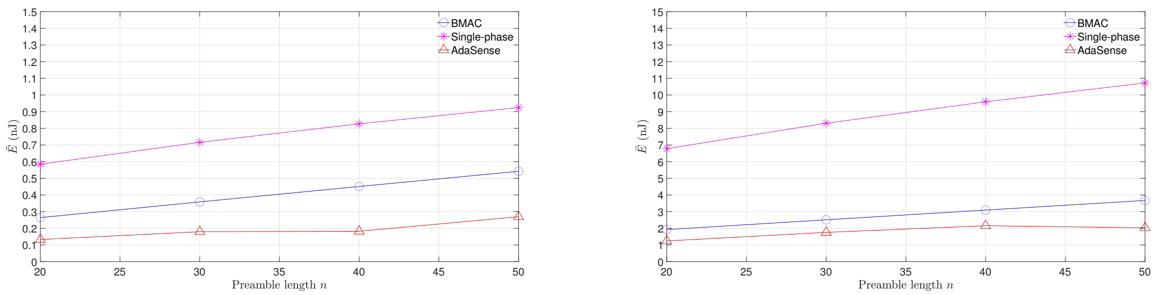

(a) $P = -60$ dBm, $P_{\text{FA}} = 10^{-3}$, $P_{\text{Miss}} = 10^{-5}$. Energy savings 50%.

(b) $P = -80$ dBm, $P_{\text{FA}} = 10^{-5}$, $P_{\text{Miss}} = 10^{-5}$. Energy savings 45%-55%.

Fig. 6: E versus n for the three different schemes with $p_1 = 10^{-10}$ and $P_{\text{Miss}} = 10^{-5}$ under two different regimes of P and P_{FA}.

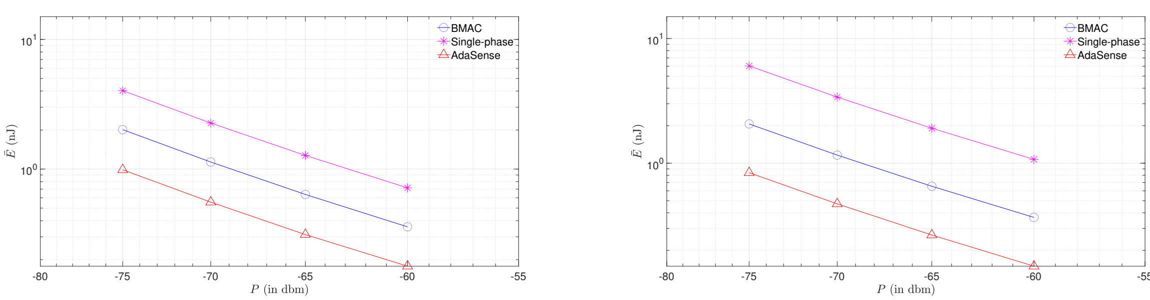

(a) $n = 30$, $P_{\text{FA}} = 10^{-3}$, $P_{\text{Miss}} = 10^{-5}$. Energy savings 50%.

(b) $n = 50$, $P_{\text{FA}} = 10^{-5}$, $P_{\text{Miss}} = 10^{-5}$. Energy savings 60%.

Fig. 7: E versus P for the three different schemes with $p_1 = 10^{-10}$ and $P_{\text{Miss}} = 10^{-5}$ under two different regimes of n and P_{FA}.

AdaSense has the smallest detection delay—this follows from the fact that both BMAC and single-phase schemes require n samples to detect a preamble, whereas AdaSense is constrained (see (9)) to take $\ell_1 + \ell_2 \leq n$ samples. Next, in Figures 5–8, we compare the exact energy consumption of the single-phase, the BMAC, and AdaSense (8)—after the optimization (9). The exact performance of these schemes are deferred to Appendix A, see Propositions 4-6. The graphs in Figures 5, 6, 7, and 8, plot the energy consumption E versus P_{Miss}, n, P, and P_{FA}, respectively, while keeping the other parameters fixed. For example, Figure 6 plots E versus n, for $P \in \{-60 \text{ dBm}, -80 \text{ dBm}\}$, $P_{\text{FA}} \in \{10^{-3}, 10^{-5}\}$, and $P_{\text{Miss}} = 10^{-5}$. The exact details of the fixed parameters appear in the captions below the figures. We further comment that these plots hold for any $p_1 < 10^{-4}$—in this range of p_1 plots remain unchanged.

As we see in Figures 5–8, AdaSense is always the most energy-efficient scheme, followed by the BMAC scheme and the single-phase scheme. Savings mostly vary around 30% to 70%, depending on the regimes of P, n, P_{FA}, and P_{Miss}, though outliers with savings as low as 13% and as high as 96% have been recorded (see Figure 8).

This article has been accepted for publication in IEEE Transactions on Green Communications and Networking. This is the author's version which has not been fully edited and content may change prior to final publication. Citation information: DOI 10.1109/TGCN.2023.3238176

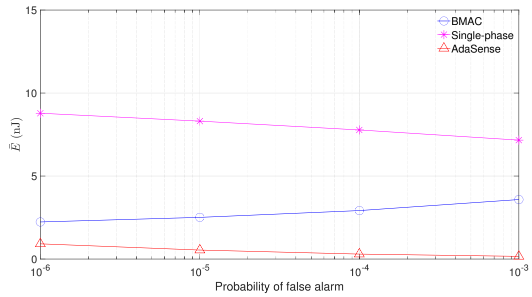

(a) $n = 30$, $P = -80$ dBm, $P_{\text{Miss}} = 10^{-5}$.
Energy savings 60%-96%.

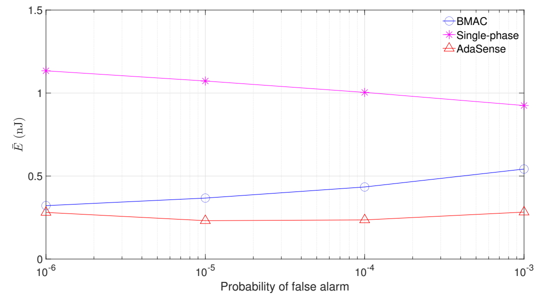

(b) $n = 50$, $P = -60$ dBm, $P_{\text{Miss}} = 10^{-5}$.
Energy savings 13%-48%.

Fig. 8: E versus P_{FA} for the three different schemes with $p_1 = 10^{-10}$ and $P_{\text{Miss}} = 10^{-5}$ under two different regimes of n and P.

Finally, for AdaSense, the numerical optimization of (9) was obtained through the MATLAB *fmincon* optimizer, using multiple initial guesses. A detailed pseudocode is available in Algorithm 1 in Appendix B. Algorithm 1 was run on an simple desktop computer (Intel®Core$^{\text{TM}}$ i5-10400 CPU @ 2.90GHz 16 GB of memory). The maximum wall-clock time needed to run the optimization was a couple of hours per set of target parameters. We remark that the time required is not an issue since the optimization in (9) needs to be run only once to set the parameters $\ell_1, \ell_2, \eta_1, \eta_2, P_{r,1}$, and $P_{r,2}$ for AdaSense.

IV. Implementation

In this section we briefly outline a possible implementation of AdaSense, see Fig. 9. The first few stages are standard for coherent receivers, which include a low noise amplifier (LNA) and a down-mixer followed by a rectifier or envelope detector and the integrator, which convert the incoming on-off keying (OOK) modulated signal to the required weighted sum $\frac{\sqrt{P}}{\sigma_{r,1}^2}\sum_{i=1}^{\ell_1} Y_i$ (see Section III) [37, Chapter 2]. This is then compared against the threshold $\eta_1 + \frac{\ell_1 P}{2\sigma_{r,1}^2}$ (see Section III) using a comparator. The heart of the architecture then lies in switching the mode of the receiver or turning it off, which is taken care of by the digital controller block.

The overhead of AdaSense with respect to a classical non-adaptive receiver is the transition between the first and the second phase. This requires modification of the noise figure (in order to switch the noise variance from $\sigma_{r,1}^2$ to $\sigma_{r,2}^2$), the integration constant which controls the weighted sum, and the threshold. There are several efficient approaches to reconfigure the receiver noise figure. Firstly, note that the Friis formula (see [38]) says that the components at the beginning of the receiver chain (*i.e.*, the radio frequency (RF) components) are the major sources of the receiver noise. The low noise amplifier (LNA) occurring at the start of the receiver chain is therefore the most suitable site to perform the noise figure reconfiguration. The simplest approach to perform this reconfiguration is to adjust the LNA's bias current. A higher bias current leads to a higher transconductance of the LNA, and hence, a better noise figure [20], but at the cost of higher power consumption. Besides the bias current readjustment method, there exists other methods to reconfigure the noise figure of the LNA as well (see [39]–[41]). The choice of the exact reconfiguration method will depend on the application and the receiver architecture. It is worth mentioning that the narrow bandwidth of the modulated signals relaxes the speed constraints on the reconfiguration and makes it easy to implement. To modify the integration constant we need to modify passive elements (capacitors or resistors). This is achieved by implementing two different values of the considered elements (resistance or capacitance) and connecting or disconnecting them using switches depending on the phase. The comparison threshold is obtained through resistive bridge dividers. To generate different comparison voltages, it suffices to add an additional resistance in the resistive ladder, which allows us to generate two comparison voltages. Depending on the phase, the comparator is connected to one or the other using switches.

V. Concluding remarks

In this paper we proposed a new channel sensing scheme, AdaSense, which is particularly energy efficient in the sparse communication regime. The main difference with existing schemes is that AdaSense adaptively chooses the number of observed samples as well as the power at which these samples are observed. We demonstrated that AdaSense provides higher energy savings than other existing channel sensing schemes, for an additive white Gaussian noise channel. Notice that the results immediately extend to the case where the thermal noise is no longer negligible—just add the thermal noise variance σ_t^2 to the receiver noise $\sigma_r^2 = f(P_r)$ throughout.

It should perhaps be emphasized that AdaSense operates only according to two power levels. In fact, one could envision a more gradual procedure where, after each observation, the receiver either stops or observes the next sample at a potentially lower noise level. Preliminary calculations reveal that the energy gains provided by such a general scheme would not be substantial compared to AdaSense. Moreover, potential energy gains would probably be offset by an increased complexity at the hardware level. Indeed, as suggested in Section IV, the implementation overhead of AdaSense with respect to a non-adaptive receiver appears to be negligible. This suggests that duty cycled receivers, including the duty-cycled *wake-up receivers* [14]–[17], could benefit from AdaSense.

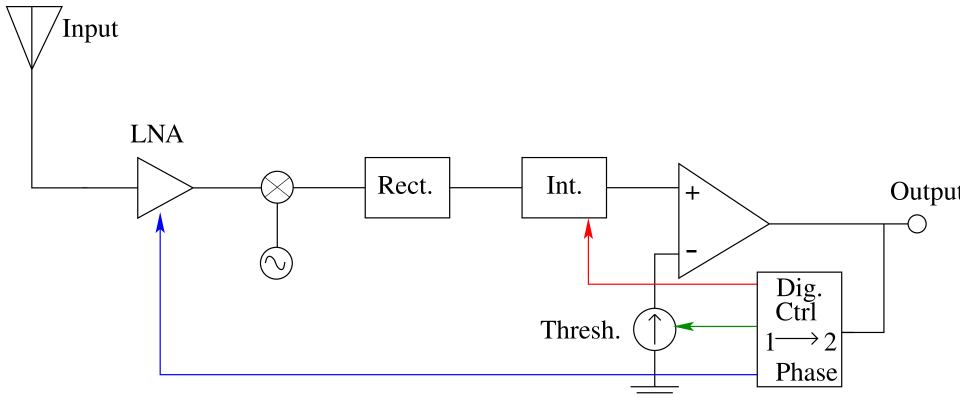

Fig. 9: AdaSense implementation

While in this paper we work with channels with fixed received power, our results and calculations can be extended to channels where the received power is a random variable, such as *fading channels*. Extension of our results are also possible to channels with multiple antennas. Even in such scenarios, AdaSense, working with multiple receiver power consumption levels, and allowed to choose the number of samples it observes adaptively, will consume lower energy than schemes with fixed power levels. We leave the task of demonstrating the exact amount of energy savings provided by AdaSense for fading and multiple antenna channels as future work. Furthermore, noting that channel sensing is a hypothesis test, a comparison of AdaSense with active hypothesis testing merits attention in the future.

Finally, regarding the physical implementation, the chosen architecture should integrate the three needed reconfigurations to switch between the two phases, i.e., i) noise figure vs power consumption reconfiguration ii) integration constant adjustment and iii) comparison threshold adjustment. A possible implementation of the receiver and the reconfigurations have been introduced in the paper. Other families of receivers could be used such as mixer-first. The choice of the best architecture should be done as a compromise between the inherent power consumption of the architecture and its suitedness to Adasense, which we leave as future work.

Appendix A
Exact analysis

According to the channel model (1), the distribution of the samples Y_i under either of the hypothesis H_0 or H_1 is i.i.d., and is given by

$$Y_i \sim \begin{cases} \mathcal{N}(0, \sigma^2), & \text{given } H_0 \\ \mathcal{N}(\sqrt{P}, \sigma^2), & \text{given } H_1. \end{cases} \tag{11}$$

Therefore, the log-likelihood ratio (LLR) of m i.i.d. samples $Y_1, Y_2, \ldots, Y_m$ is given by

$$\begin{aligned} T &= \log\left(\frac{\prod_{i=1}^m \frac{1}{\sqrt{2\pi\sigma^2}} \exp\{-\frac{1}{2\sigma^2}(Y_i - \sqrt{P})^2\}}{\prod_{i=1}^m \frac{1}{\sqrt{2\pi\sigma^2}} \exp\{-\frac{1}{2\sigma^2}(Y_i)^2\}} \right) \\ &= \frac{\sqrt{P}}{\sigma^2} \sum_{i=1}^m Y_i - \frac{mP}{2\sigma^2}. \end{aligned} \tag{12}$$

Hence,

$$T \sim \begin{cases} \mathcal{N}\left(-\frac{mP}{2\sigma^2}, \frac{mP}{\sigma^2}\right) & \text{given } H_0 \\ \mathcal{N}\left(\frac{mP}{2\sigma^2}, \frac{mP}{\sigma^2}\right) & \text{given } H_1. \end{cases} \tag{13}$$

The next three propositions state the performance of the single-phase scheme, the BMAC scheme, and AdaSense, in the non-asymptotic regime.

Proposition 4 is textbook material (see, *e.g.*, [30, Example II.D.1]) and follows from (12) and (13):

Proposition 4. *Given n, P, $\sigma_r^2 = f(P_r)$, the single-phase scheme achieves*

$$P_{FA} = Q\left(\frac{\sigma_r \eta}{\sqrt{nP}} + \frac{1}{2}\sqrt{\frac{nP}{\sigma_r^2}}\right),$$

$$\textit{and } P_{Miss} = Q\left(-\frac{\sigma_r \eta}{\sqrt{nP}} + \frac{1}{2}\sqrt{\frac{nP}{\sigma_r^2}}\right).$$

The energy consumed by the receiver is[9]

$$E = nP_r. \tag{14}$$

Proposition 5 (BMAC)**.** *Given p_1, n, P, $\sigma_r^2 = f(P_r)$, the BMAC scheme achieves*

$$P_{FA} = P_{e,0}^n,$$

$$\textit{and } P_{Miss} = 1 - (1 - P_{e,1})^n,$$

where $P_{e,0} = Q(\frac{\eta}{\sigma_r})$, $P_{e,1} = 1 - Q(\frac{\eta - \sqrt{P}}{\sigma_r})$, with $\eta \in \mathbb{R}$. The average energy consumed by the BMAC scheme is

$$\begin{aligned} E &= P_r \left[\frac{p_1 P_{Miss}}{1 - (1 - P_{Miss})^{1/n}} + \frac{(1 - p_1)(1 - P_{FA})}{1 - P_{FA}^{1/n}} \right] \\ &= P_r \frac{(1 - P_{FA})}{1 - P_{FA}^{1/n}} + o(1) \end{aligned} \tag{15}$$

where $o(1)$ tends to zero as $p_1 \to 0$.

Note that given p_1, n, and P, fixing any two values among P_{FA}, P_{Miss}, and E specifies the third one.

[9]Recall that the transmitted symbols have unit duration.

This article has been accepted for publication in IEEE Transactions on Green Communications and Networking. This is the author's version which has not been fully edited and content may change prior to final publication. Citation information: DOI 10.1109/TGCN.2023.3238176

Proof of Proposition 5: We have

$$\begin{aligned} P_{\text{FA}} &= \Pr(\widehat{M}=1|H_0) \\ &= \prod_{i=1}^{n} \Pr(Y_i > \eta | H_0) \quad (16)\\ &= Q\left(\frac{\eta}{\sigma_r}\right)^n, \quad (17) \end{aligned}$$

where (16) follows from the fact that the BMAC detection rule declares $\widehat{M}=1$ if and only if $Y_i > \eta$ for $i \in \{1,\dots,n\}$ and where (17) follows from (11). Similarly, we have

$$\begin{aligned} P_{\text{Miss}} &= \Pr(\widehat{M}=0|H_1) \\ &= 1-\prod_{i=1}^{n} \Pr(Y_i > \eta | H_1) \quad (18)\\ &= 1-Q\left(\frac{\eta-\sqrt{P}}{\sigma_r}\right)^n. \quad (19) \end{aligned}$$

For the average energy consumption E we have

$$\begin{aligned} E &= \sum_{i=1}^{n} iP_r \Pr(N=i) \\ &= \sum_{i=1}^{n} iP_r \Big[p_1 \Pr(N=i|H_1) + (1-p_1)\Pr(N=i|H_0)\Big]. \end{aligned} \quad (20)$$

We now calculate $\Pr(N=i|H_0)$. For $i<n$, note that $N=i$ if and only if $Y_j > \eta$ for all $j<i$, and $Y_i \le \eta$. Thus, by (11), we have

$$\Pr(N=i|H_0) = Q\left(\frac{\eta}{\sigma_r}\right)^{i-1}\left(1-Q\left(\frac{\eta}{\sigma_r}\right)\right).$$

On the other hand, $N=n$ occurs if and only if $Y_j > \eta$ for all $j<n$. Therefore, $\Pr(N=n|H_0) = Q\left(\frac{\eta}{\sigma_r}\right)^{n-1}$. Similarly, we have

$$\Pr(N=i|H_1) = Q\left(\frac{\eta-\sqrt{P}}{\sigma_r}\right)^{i-1}\left(1-Q\left(\frac{\eta-\sqrt{P}}{\sigma_r}\right)\right),$$

for all $i<n$, and

$$\Pr(N=n|H_1) = Q\left(\frac{\eta-\sqrt{P}}{\sigma_r}\right)^{n-1}.$$

Define $p \triangleq Q\left(\frac{\eta}{\sigma_r}\right)$ and $q \triangleq Q\left(\frac{\eta-\sqrt{P}}{\sigma_r}\right)$. Then, using (20)

$$\begin{aligned} E &= \sum_{i=1}^{n-1} iP_r\Big[p_1 q^{i-1}(1-q) + (1-p_1)p^{i-1}(1-p)\Big] \\ &\quad + nP_r\Big[p_1 q^{n-1} + (1-p_1)p^{n-1}\Big] \\ &= P_r\Big[p_1 \sum_{i=0}^{n-1} q^i + (1-p_1)\sum_{i=0}^{n-1} p^i\Big] \\ &= P_r\Big[p_1 \frac{1-q^n}{1-q} + (1-p_1)\frac{1-p^n}{1-p}\Big] \\ &= P_r\Big[p_1 \frac{P_{\text{Miss}}}{1-(1-P_{\text{Miss}})^{1/n}} + (1-p_1)\frac{1-P_{\text{FA}}}{1-P_{\text{FA}}^{1/n}}\Big], \quad (21) \end{aligned}$$

where (21) follows from the definitions of p and q together with (17) and (19). ■

Proposition 6 (AdaSense)**.** *Given p_1, n, P, $\sigma_r^2 = f(P_r)$, the first and second phase lengths $\ell_1, \ell_2 \ge 0$ such that $\ell_1+\ell_2 \le n$, the powers in the first and second phases $P_{r,1}, P_{r,2} \ge 0$, and the thresholds of the hypothesis tests of the first and second phases $\eta_1, \eta_2 \in \mathbb{R}$, AdaSense yields*

$$P_{FA} = Q\left(\frac{\sigma_{r,1}\eta_1}{\sqrt{\ell_1 P}} + \frac{1}{2}\sqrt{\frac{\ell_1 P}{\sigma_{r,1}^2}}\right) Q\left(\frac{\sigma_{r,2}\eta_2}{\sqrt{\ell_2 P}} + \frac{1}{2}\sqrt{\frac{\ell_2 P}{\sigma_{r,2}^2}}\right),$$

and

$$\begin{aligned} P_{Miss} &= Q\left(-\frac{\sigma_{r,1}\eta_1}{\sqrt{\ell_1 P}} + \frac{1}{2}\sqrt{\frac{\ell_1 P}{\sigma_{r,1}^2}}\right) \\ &\quad + \left(1-Q\left(-\frac{\sigma_{r,1}\eta_1}{\sqrt{\ell_1 P}} + \frac{1}{2}\sqrt{\frac{\ell_1 P}{\sigma_{r,1}^2}}\right)\right) \\ &\quad \times Q\left(-\frac{\sigma_{r,2}\eta_2}{\sqrt{\ell_2 P}} + \frac{1}{2}\sqrt{\frac{\ell_2 P}{\sigma_{r,2}^2}}\right), \end{aligned}$$

The average energy consumed is given by

$$E = \ell_1 P_{r,1} + p_c \ell_2 P_{r,2}, \quad (22)$$

where

$$\begin{aligned} p_c &= (1-p_1) Q\left(\frac{\sigma_{r,1}\eta_1}{\sqrt{\ell_1 P}} + \frac{1}{2}\sqrt{\frac{\ell_1 P}{\sigma_{r,1}^2}}\right) \\ &\quad + p_1\left(1-Q\left(-\frac{\sigma_{r,1}\eta_1}{\sqrt{\ell_1 P}} + \frac{1}{2}\sqrt{\frac{\ell_1 P}{\sigma_{r,1}^2}}\right)\right) \\ &= Q\left(\frac{\sigma_{r,1}\eta_1}{\sqrt{\ell_1 P}} + \frac{1}{2}\sqrt{\frac{\ell_1 P}{\sigma_{r,1}^2}}\right) + o(1), \end{aligned}$$

where $o(1)$ tends to zero as p_1 tends to zero.

Proof of Proposition 6: We begin by evaluating the LLR for samples in the first and the second phases. Recall that the first batch of ℓ_1 samples are received with noise variance $\sigma_{r,1}^2 = f(P_{r,1})$, while the second batch of ℓ_2 samples are received with noise variance $\sigma_{r,2}^2 = f(P_{r,2})$. Let T_1 and T_2 denote the LLRs of the samples in the first and the second phases, respectively. By (12), we have

$$\begin{aligned} T_1 &= \frac{\sqrt{P}}{\sigma_{r,1}^2}\sum_{i=1}^{\ell_1} Y_i - \frac{\ell_1 P}{2\sigma_{r,1}^2}, \\ T_2 &= \frac{\sqrt{P}}{\sigma_{r,2}^2}\sum_{i=\ell_1+1}^{\ell_1+\ell_2} Y_i - \frac{\ell_2 P}{2\sigma_{r,2}^2}. \end{aligned} \quad (23)$$

From (13)

$$T_1 \sim \begin{cases} \mathcal{N}\left(-\frac{\ell_1 P}{2\sigma_{r,1}^2}, \frac{\ell_1 P}{\sigma_{r,1}^2}\right) & \text{given } H_0 \\ \mathcal{N}\left(\frac{\ell_1 P}{2\sigma_{r,1}^2}, \frac{\ell_1 P}{\sigma_{r,1}^2}\right) & \text{given } H_1, \end{cases} \quad (24)$$

and

$$T_2 \sim \begin{cases} \mathcal{N}\left(-\frac{\ell_2 P}{2\sigma_{r,2}^2}, \frac{\ell_2 P}{\sigma_{r,2}^2}\right) & \text{given } H_0 \\ \mathcal{N}\left(\frac{\ell_2 P}{2\sigma_{r,2}^2}, \frac{\ell_2 P}{\sigma_{r,2}^2}\right) & \text{given } H_1. \end{cases} \tag{25}$$

Note that T_1 and T_2 are independent since they are functions of different sets of samples.

We now proceed to evaluate P_{FA} and P_{Miss}. Note that $\widehat{M} = 1$, if and only if $T_1 > \eta_1$ and $T_2 > \eta_2$. Therefore,

$$P_{\text{FA}} = \Pr(T_1 > \eta_1 | H_0) \Pr(T_2 > \eta_2 | H_0) \tag{26}$$

$$= Q\left(\frac{\sigma_{r,1}\eta_1}{\sqrt{\ell_1 P}} + \frac{1}{2}\sqrt{\frac{\ell_1 P}{\sigma_{r,1}^2}}\right) Q\left(\frac{\sigma_{r,2}\eta_2}{\sqrt{\ell_2 P}} + \frac{1}{2}\sqrt{\frac{\ell_2 P}{\sigma_{r,2}^2}}\right), \tag{27}$$

where the second equality follows from (24) and (25). Similarly, we have

$$\begin{aligned} P_{\text{Miss}} &= \Pr(T_1 \le \eta_1 | H_1) + \Pr(T_1 > \eta_1 | H_1) \Pr(T_2 \le \eta_2 | H_1) \\ &= Q\left(-\frac{\sigma_{r,1}\eta_1}{\sqrt{\ell_1 P}} + \frac{1}{2}\sqrt{\frac{\ell_1 P}{\sigma_{r,1}^2}}\right) \\ &\quad + \left(1 - Q\left(-\frac{\sigma_{r,1}\eta_1}{\sqrt{\ell_1 P}} + \frac{1}{2}\sqrt{\frac{\ell_1 P}{\sigma_{r,1}^2}}\right)\right) \\ &\quad \times Q\left(-\frac{\sigma_{r,2}\eta_2}{\sqrt{\ell_2 P}} + \frac{1}{2}\sqrt{\frac{\ell_2 P}{\sigma_{r,2}^2}}\right). \end{aligned}$$

Next, we compute the average energy consumption E. We have

$$E = \ell_1 P_{r,1} + p_c \ell_2 P_{r,2}$$

where p_c denotes the probability that the scheme continues after the first phase by p_c, that is $T_1 > \eta_1$. From (24), we have

$$p_c = (1 - p_1)\Pr(T_1 > \eta_1 | H_0) + p_1 \Pr(T_1 > \eta_1 | H_1)$$

$$= (1 - p_1) Q\left(\frac{\sigma_{r,1}\eta_1}{\sqrt{\ell_1 P}} + \frac{1}{2}\sqrt{\frac{\ell_1 P}{\sigma_{r,1}^2}}\right) \tag{28}$$

$$+ p_1 \left(1 - Q\left(-\frac{\sigma_{r,1}\eta_1}{\sqrt{\ell_1 P}} + \frac{1}{2}\sqrt{\frac{\ell_1 P}{\sigma_{r,1}^2}}\right)\right). \tag{29}$$

which concludes the proof. ■

Appendix B
Pseudocode to obtain the optimal parameters for AdaSense using fmincon

In this section, we provide the pseudocode used to numerically solve the optimization in (9) needed to set the parameters $\ell_1, \ell_2, \eta_1, \eta_2, P_{r,1}, P_{r,2}$ of AdaSense, for a given n, P, p_1, α, and β. As described in Section III, the optimization in (9) is non-convex, and hence we resort to obtain a 'good-enough' feasible point using MATLAB's built-in fmincon optimizer. The fmincon module however performs local optimization starting with a single initial guess. Since the objective function and the constraints in (9) are highly non-convex, we run multiple instances of fmincon initiated at different points, and choose the best possible feasible choice, *i.e.,* the one with the least energy consumption, across all possible instances.

In more detail, for the initialization, we chose two possible values for all parameters except $P_{r,1}$ and four possible values for $P_{r,1}$. In total, this gave us $2^5 \times 4 = 128$ different initial points. We initiated the fmincon solver at each of these initial points, and returned the results of the one which gave a feasible point with the least energy. The details are available in Algorithm 1.

Appendix C
Asymptotics

Proof of Theorem 2 (Single-phase): From Stein's Lemma [32, Theorem 11.8.3], if the single-phase satisfies $P_{\text{Miss}} \le \beta$, for some fixed $0 < \beta < 1$, then[10]

$$\begin{aligned} P_{\text{FA}} &= \exp\left(-\frac{P}{2}\frac{1}{\sigma_r^2} n \pm o(n)\right) \\ &= \exp\left(-\frac{P}{2k} P_r^{\gamma} n \pm o(n)\right) \\ &= \exp\left(-\frac{P P_r^{\gamma-1}}{2k} E \pm o(E)\right) \end{aligned} \tag{30}$$

where for the first inequality we used the noise profile $\sigma_r^2 = k P_r^{-\gamma}$ and where the second inequality holds since $E = n P_r$ (see (14)). Therefore,

$$E = \frac{2k}{P P_r^{\gamma-1}(1 \pm o(1))} \ln(1/P_{\text{FA}})$$

where $o(1)$ vanishes as $P_{\text{FA}} \to 0$—notice that as $P_{\text{FA}} \to 0$ we necessarily have n and E tend to infinity. ■

Notice that the proof of Theorem 2 also holds if $0 < \gamma < 1$. The same comment goes for the proof of Theorem 3 (see below). We nevertheless chose to state these theorems by restricting $\gamma \ge 1$ for the sake of uniformity with Theorem 1 and since the case $\gamma < 1$ is less natural as previously alluded to.

Proof of Theorem 1 (AdaSense): By Proposition 6

$$E = E_1 + E_2 p_c \tag{31}$$

where

$$E_i = \ell_i P_{r,i} \quad i = 1, 2$$

denotes the energy spent during the first and the second phase, and where p_c denotes the probability that AdaSense performs the second phase, *i.e.,* $p_c = \Pr(T_1 > \eta_1)$.

Now pick $0 < \varepsilon < 1$ and let us allocate the energy E of the first and the second phase as

$$E_1 = \varepsilon E = \ell_1 P_{r,1}$$

and

$$E_2 = \frac{(1 - \varepsilon)E}{p_c} = \ell_2 P_{r,2} \tag{32}$$

Furthermore, pick

$$\ell_i = \delta_i n \qquad i = 1, 2 \tag{33}$$

[10]We write $f(n) = g(n) \pm q(n)$ if $g(n) - q(n) \le f(n) \le g(n) + q(n)$.

This article has been accepted for publication in IEEE Transactions on Green Communications and Networking. This is the author's version which has not been fully edited and content may change prior to final publication. Citation information: DOI 10.1109/TGCN.2023.3238176

Algorithm 1 Optimization for AdaSense in (9)

Input: n, P, α, β, p_1

$\ell_1^{(i)} \leftarrow [\ell_{1_j}^{(i)} : 1 \leq j \leq k_1]$, $\ell_2^{(i)} \leftarrow [\ell_{2_j}^{(i)} : 1 \leq j \leq k_2]$, $\eta_1^{(i)} \leftarrow [\eta_{1_j}^{(i)} : 1 \leq j \leq k_3]$, $\eta_2^{(i)} \leftarrow [\eta_{2_j}^{(i)} : 1 \leq j \leq k_4]$, $P_{r,1}^{(i)} \leftarrow [P_{r,1_j}^{(i)} : 1 \leq j \leq k_5]$, $s^{(i)} \leftarrow [s_j^{(i)} : 1 \leq j \leq k_6]$
▷ Initial values of $\ell_1, \ell_2, \eta_1, \eta_2, P_{r,1}, s \triangleq \frac{P_{r,2}}{P_{r,1}}$ for starting fmincon.

flag$\leftarrow 0$; ▷ Variable indicating whether feasible solution is found
val$\leftarrow 0$;

for $j_1 = 1 : k_1$ **do**
  for $j_2 = 1 : k_2$ **do**
    for $j_3 = 1 : k_3$ **do**
      for $j_4 = 1 : k_4$ **do**
        for $j_5 = 1 : k_5$ **do**
          for $j_6 = 1 : k_6$ **do**
            init$\leftarrow [\ell_{1_{j_1}}^{(i)}, \ell_{2_{j_2}}^{(i)}, \eta_{1_{j_3}}^{(i)}, \eta_{2_{j_4}}^{(i)}, P_{r,1_{j_5}}^{(i)}, s_{j_6}^{(i)}]$; ▷ The initial guess for the optimization
            $\tilde{\ell}_1, \tilde{\ell}_2, \tilde{\eta}_1, \tilde{\eta}_2, \tilde{P}_{r,1}, \tilde{s} \leftarrow$OPTIMIZE(init);
            ▷ Optimization in (9) using fmincon. Returns the best possible argument as obtained by fmincon.
            con1$\leftarrow \mathbf{1}\{\tilde{\ell}_1 + \tilde{\ell}_2 - n \leq 0\}$;
            con2$\leftarrow \mathbf{1}\{P_{\text{FA}} \leq \alpha\}$;
            ▷ P_{FA} is calculated according to (6) using $\tilde{\ell}_1, \tilde{\ell}_2, \tilde{\eta}_1, \tilde{\eta}_2, \tilde{P}_{r,1}, \tilde{s}$
            con3$\leftarrow \mathbf{1}\{P_{\text{Miss}} \leq \beta\}$;
            ▷ P_{Miss} is calculated according to (7) using $\tilde{\ell}_1, \tilde{\ell}_2, \tilde{\eta}_1, \tilde{\eta}_2, \tilde{P}_{r,1}, \tilde{s}$
            $E \leftarrow \tilde{\ell}_1 \tilde{P}_{r,1} + p_c \tilde{\ell}_2 \tilde{P}_{r,2}$; ▷ Computing E according to (8)
            if con1$==1$ && con2$==1$ && con3$==1$ **then**
            ▷ Checking if the returned solution satisfies the constraint in (9)
              if flag$==0$ **then**
                val$\leftarrow E$;
                $\ell_1^*, \ell_2^*, \eta_1^*, \eta_2^*, P_{r,1}^*, s^* \leftarrow \tilde{\ell}_1, \tilde{\ell}_2, \tilde{\eta}_1, \tilde{\eta}_2, \tilde{P}_{r,1}, \tilde{s}$;
                flag$\leftarrow 1$;
              end if
              if $E <$ val **then**
                val$\leftarrow E$;
                $\ell_1^*, \ell_2^*, \eta_1^*, \eta_2^*, P_{r,1}^*, s^* \leftarrow \tilde{\ell}_1, \tilde{\ell}_2, \tilde{\eta}_1, \tilde{\eta}_2, \tilde{P}_{r,1}, \tilde{s}$;
              end if
            end if
          end for
        end for
      end for
    end for
  end for
end for
if flag$==0$ **then**
  return ‘No feasible point found’
else
  return $\ell_1^*, \ell_2^*, \eta_1^*, \eta_2^*, P_{r,1}^*, s^*$
end if

such that $\delta_1 > 0$, $\min\{E_2/n, \varepsilon\} \leq \delta_2 \leq 1-\varepsilon$, and $\delta_1+\delta_2 \leq 1$. As we will see below, the tradeoff between P_{FA} and E is improved as ε gets smaller, that is when the overwhelming energy is spent during the second phase.

From Stein's Lemma [32, Theorem 11.8.3] it follows that for any $\beta > 0$, the thresholds η_1, η_2 may be set such that $P_{\text{Miss}} \leq \beta$ and such that

$$\Pr(T_i > \eta_i | H_0) \leq \exp\left(-\frac{P}{2}\frac{1}{\sigma_{r,i}^2}\ell_i + o(\ell_i)\right) \quad i = 1, 2. \tag{34}$$

Hence, from (26)

$$\begin{aligned} P_{\text{FA}} &\leq \exp\left(-\frac{P}{2}\frac{1}{\sigma_{r,2}^2}\ell_2 + o(\ell_2)\right) \\ &= \exp\left(-\frac{P}{2k}P_{r,2}^{\gamma}\delta_2 n + o(n)\right) \end{aligned} \tag{35}$$

where for the second equality we used (33) and the noise profile $\sigma_r^2 = kP_r^{-\gamma}$. We now consider the problem of minimizing the first term in the exponent on the right-hand side of (35) under the constraints (32)-(33), that is

$$\max_{\substack{(P_{r,2},\delta_2):\\ \min\{E_2/n,\varepsilon\}\leq\delta_2\leq 1-\varepsilon \\ P_{r,2}\delta_2 = E_2/n}} P_{r,2}^{\gamma}\delta_2 \tag{36}$$

and distinguish the cases $\gamma = 1$ and $\gamma > 1$.

$\gamma = 1$: In this case (36) is equal to $(1-\varepsilon)E/np_c$ which together with (35) yields

$$P_{\text{FA}} \leq \exp\left(-\frac{(1-\varepsilon)P}{2kp_c}E(1+o(1))\right) \tag{37}$$

where $o(1)$ tends to zero as E tends to infinity. Hence,

$$E \leq p_c \frac{2k(1+o(1))}{P(1-\varepsilon)}\ln\left(\frac{1}{P_{\text{FA}}}\right) \tag{38}$$

where $o(1)$ tends to zero as P_{FA} tends to zero.

$\gamma > 1$: Here we obtain a tradeoff between energy and probability of false-alarm which is at least as good as for $\gamma = 1$. To see this suppose $n\delta_2 P_{r,2} = E_2$ and pick $\delta_2 > 0$ small enough so that $P_{r,2} \geq 1$ (this is possible since by assumption δ_2 can be taken as small as $\min\{\varepsilon, E_2/n\} \leq E_2/n$). Then $P_{r,2}^{\gamma} \geq P_{r,2}$ and we deduce that (36) is greater or equal to E_2/n. Hence (38) also holds if $\gamma > 1$.

We now upper bound p_c as

$$\begin{aligned} p_c &= \Pr(T_1 > \eta_1 | H_0)(1-p_1) + \Pr(T_1 > \eta_1 | H_1)p_1 \\ &\leq \Pr(T_1 > \eta_1 | H_0) + p_1 \\ &\leq p_1 + o(1) \end{aligned} \tag{39}$$

where $o(1)$ tends to zero as n tends to infinity (or, equivalently, as P_{FA} tends to zero), and where for the last inequality we used (34) and the fact that ℓ_1 increases with n. The theorem then follows from (38) and (39). ■

Proof of Theorem 3: From Proposition 5, if BMAC satisfies $P_{\text{FA}} = \alpha$ and $P_{\text{Miss}} = \beta$, then

$$\alpha = Q\left(\frac{\eta}{\sigma_r}\right)^n \tag{40}$$

$$(1-\beta) = Q\left(\frac{\eta - \sqrt{P}}{\sigma_r}\right)^n \tag{41}$$

$$E \geq P_r \frac{(1-p_1)(1-\alpha)}{1-\alpha^{1/n}}. \tag{42}$$

From (40), the noise profile $\sigma_r^2 = kP_r^{-\gamma}$, and the Chernoff approximation on the Q-function $Q(x) = \exp(-x^2/2(1+o(1)))$ as $x \to \infty$ we deduce that

$$P_r = \left(\frac{\sqrt{k}Q^{-1}(\alpha^{1/n})}{\eta}\right)^{2/\gamma} = \left(\frac{2k}{n\eta^2(1+o(1))}\ln(1/\alpha)\right)^{1/\gamma} \tag{43}$$

where $o(1) \to 0$ as $\alpha \to 0$. Hence, from (42)

$$E \geq \frac{(1-p_1)(1-\alpha)}{1-\alpha^{1/n}}\left(\frac{2k}{n\eta^2(1+o(1))}\ln(1/\alpha)\right)^{1/\gamma} \tag{44}$$

Assuming $\beta < 1/2$ we necessarily have $\eta \leq \sqrt{P}$ from (41) and we finally get[11]

$$E \geq (1-p_1)\left(\frac{2k}{nP}\ln(1/\alpha)\right)^{1/\gamma}(1-o(1)). \tag{45}$$

as $\alpha \to 0$. ■

REFERENCES

[1] E. Sasmita, M. Rosmiati, and M. Rizal, "Integrating forest fire detection with wireless sensor network based on long range radio," in *Int. Conf. on Control, Electronics, Renewable Energy and Communications (ICCEREC)*, 2018, pp. 222–225.

[2] S. Ananth, P. Sathya, and P. Madhan Mohan, "Smart health monitoring system through IoT," in *IEEE Int. Conf. on Comm. and Signal Processing ICCSP*, 2019, pp. 968–970.

[3] G. Picco *et al.*, "Geo-referenced proximity detection of wildlife with WildScope: Design and characterization," in *Int. Conf. on Inf. Processing Sensor Netw. (IPSN)*, 2015, pp. 238–249.

[4] D. Ciuonzo, P. S. Rossi, and P. K. Varshney, "Distributed detection in wireless sensor networks under multiplicative fading via generalized score tests," *IEEE Internet of Things Journal*, vol. 8, no. 11, pp. 9059–9071, 2021.

[5] S. A. Aldalahmeh and D. Ciuonzo, "Distributed detection fusion in clustered sensor networks over multiple access fading channels," *IEEE Transactions on Signal and Information Processing over Networks*, vol. 8, pp. 317–329, 2022.

[6] C. Li, G. Li, and P. K. Varshney, "Distributed detection of sparse signals with censoring sensors in clustered sensor networks," *Information Fusion*, vol. 83-84, pp. 1–18, 2022. [Online]. Available: https://www.sciencedirect.com/science/article/pii/S1566253522000276

[7] J. Suh and M. Horton, "Powering sensor networks," *IEEE Potentials*, vol. 23, no. 3, pp. 35–38, 2004.

[8] M. Barnett, D. Bruck, and A. Jago, "Mean annual probability of having a residential fire experience throughout a lifetime: Development and application of a methodology," in *Proc. of the Asia-Oceania Symp. on Fire Science & Technology*, 2007.

[9] A. El-Hoiydi, J.-D. Decotignie, and J. Hernandez, "Low power mac protocols for infrastructure wireless sensor networks," in *Proc. of the Fifth European Wireless Conference*, 2004.

[10] W. Ye, J. S. Heidemann, and E. Estrin, "An energy-efficient mac protocol for wireless sensor networks," in *Proc. of the 21st Int. Annual Joint Conf. of the IEEE Computer and Communications Societies (INFOCOM 2002)*, 2002, pp. 1567–1576.

[11] T. van Dam and K. Langendoen, "An adaptive energy-efficient mac protocol for wireless sensor networks," in *Proc. of the 1st Int. Conf. on Embedded Networked Sensor Systems*, 2003, pp. 171–180.

[12] J. Polastre, J. Hill, and D. Culler, "Versatile low power media access for wireless sensor networks," in *Proc. of the 2nd Int. Conf. on Embedded Networked Sensor Systems*, 2004, pp. 95–107.

[11] Notice that $\eta \leq \sqrt{P}$ is a crude bound and is definitely not sufficient to have $\beta < 1/2$ as even for $\eta = \sqrt{P}$ we have $\beta = 1 - (1/2)^n \geq 1/2$.

[13] M. Buettner, G. V. Yee, E. Anderson, and R. Han, "X-MAC: A short preamble mac protocol for duty-cycled wireless sensor networks," in *Proc. of the 4th Int. Conf. on Embedded Networked Sensor Systems*, 2006, pp. 307–320.

[14] N. Mazloum and O. Edfors, "Performance analysis and energy optimization of wake-up receiver schemes for wireless low-power applications," *IEEE Trans. on Wireless Comm.*, vol. 13, pp. 7050–7061, 12 2014.

[15] S. Bdiri, F. Derbel, and O. Kanoun, "A tuned-rf duty-cycled wake-up receiver with −90 dbm sensitivity," *Sensors*, vol. 18, 2018.

[16] N. Mazloum and O. Edfors, "DCW-MAC: An energy efficient medium access scheme using duty-cycled low-power wake-up receivers," in *Proc. of the 74th IEEE Vehicular Technology Conference*, September 2011, pp. 1–5.

[17] N. Seyed Mazloum and O. Edfors, "Influence of duty-cycled wake-up receiver characteristics on energy consumption in single-hop networks," *IEEE Transactions on Wireless Communications*, vol. 16, no. 6, pp. 3870–3884, June 2017.

[18] J. L. Hill and D. E. Culler, "Mica: A wireless platform for deeply embedded networks," *IEEE Micro*, vol. 22, no. 6, pp. 12–24, Nov. 2002.

[19] A. El-Hoiydi, "Aloha with preamble sampling for sporadic traffic in ad hoc wireless sensor networks," in *Proc. of IEEE Int. Conf. on Communication (ICC)*, 2002, pp. 3418–3423.

[20] T. H. Lee, *The Design of CMOS Radio-Frequency Integrated Circuits*. Cambridge University Press, 2004.

[21] T. Banerjee and V. V. Veeravalli, "Data-efficient quickest change detection in minimax settings," *IEEE Transactions on Information Theory*, vol. 59, no. 10, pp. 6917–6931, 2013.

[22] A. Tchamkerten, V. Chandar, and G. Caire, "Energy and sampling constrained asynchronous communication," *IEEE Transactions on Information Theory*, vol. 60, no. 12, pp. 7686–7697, 2014.

[23] E. Ebrahimzadeh and A. Tchamkerten, "Sequential detection of transient changes in stochastic systems under a sampling constraint," in *2015 IEEE International Symposium on Information Theory (ISIT)*. IEEE, 2015, pp. 156–160.

[24] V. Chandar and A. Tchamkerten, "Sampling constrained asynchronous communication: How to sleep efficiently," *IEEE Trans. on Inf. Theory*, vol. 64, pp. 1867–1878, 3 2018.

[25] J. Xie and J. Chen, "An adaptive double-threshold spectrum sensing algorithm under noise uncertainty," in *2012 IEEE 12th International Conference on Computer and Information Technology*, 2012, pp. 824–827.

[26] M. Lai, S. Peng, X. Yang, and L. Zhou, "Fast two-step energy detection for spectrum sensing," *Journal of Electrical and Computer Engineering*, vol. 2015, pp. 1–6, 01 2015.

[27] T. Yang, Y. Wu, L. Li, W. Xu, and W. Tan, "A two-step cooperative energy detection algorithm robust to noise uncertainty," *Wirel. Commun. Mob. Comput.*, vol. 2019, 2019.

[28] R. Piyare, A. Murphy, C. Kiraly, P. Tosato, and D. Brunelli, "Ultra low power wake-up radios: A hardware and networking survey," *IEEE Comm. Surveys & Tutorials*, vol. 19, no. 4, pp. 2117–2157, 2017.

[29] A. Klenke, *Probability Theory: A Comprehensive Course*, ser. Universitext. Springer London, 2007. [Online]. Available: https://books.google.co.in/books?id=tcm3y5UJxDsC

[30] H. V. Poor, *An Introduction to Signal Detection and Estimation (2nd Ed.)*. Berlin, Heidelberg: Springer-Verlag, 1994.

[31] S. Boyd and L. Vandenberghe, *Convex Optimization*. Cambridge University Press, 2004.

[32] T. M. Cover and J. A. Thomas, *Elements of Information Theory*. USA: Wiley-Interscience, 2006.

[33] T. Abe, T. Morie, K. Satou, D. Nomasaki, S. Nakamura, Y. Horiuchi, and K. Imamura, "An ultra-low-power 2-step wake-up receiver for IEEE 802.15.4g wireless sensor networks," in *2014 Symp. on VLSI Circuits Digest of Technical Papers*, 2014, pp. 1–2.

[34] T. Honjo, H. Yamato, T. Mikami, and C. Grimmond, "Network optimization for enhanced resilience of urban heat island measurements," *Sustainable Cities and Society*, vol. 19, pp. 319 – 330, 2015.

[35] E. Nilsson and C. Svensson, "Power consumption of integrated low-power receivers," *IEEE Journal on Emerging and Selected Topics in Circuits and Systems*, vol. 4, pp. 273–283, 09 2014.

[36] "IEEE Standard for Low-Rate Wireless Networks," *IEEE Std 802.15.4™-2015*, 2015.

[37] A. J. Viterbi and J. K. Omura, *Principles of Digital Communication and Coding*, 1st ed. New York, NY, USA: McGraw-Hill, Inc., 1979.

[38] H. Friis, "Noise figures of radio receivers," in *Proc. of the IRE*, vol. 32, no. 7, 1944, pp. 419–422.

[39] S. Chen and K. Cheng, "A 433 mhz 54 μw ook/fsk/psk compatible wake-up receiver with 11 μw low-power mode based on injection-locked oscillator," in *ESSCIRC Conference 2016: 42nd European Solid-State Circuits Conference*, Sep. 2016, pp. 137–140.

[40] X. Huang, P. Harpe, G. Dolmans, and H. de Groot, "A 915mhz ultra-low power wake-up receiver with scalable performance and power consumption," in *2011 Proceedings of the ESSCIRC (ESSCIRC)*, Sep. 2011, pp. 543–546.

[41] P. P. Wang, H. Jiang, L. Gao, P. Sen, Y. Kim, G. M. Rebeiz, P. P. Mercier, and D. A. Hall, "A near-zero-power wake-up receiver achieving −69-dbm sensitivity," *IEEE Journal of Solid-State Circuits*, vol. 53, no. 6, pp. 1640–1652, June 2018.